Structural and magnetic phase transitions in the ternary iron arsenides $SrFe_2As_2$ and $EuFe_2As_2$

FAST TRACK COMMUNICATION

Structural and magnetic phase transitions in the ternary iron arsenides SrFe$_2$As$_2$ and EuFe$_2$As$_2$

Marcus Tegel[1], Marianne Rotter[1], Veronika Weiß[1], Falko M Schappacher[2], Rainer Pöttgen[2] and Dirk Johrendt[1]

[1] Department Chemie und Biochemie der Ludwig-Maximilians-Universität München, Butenandtstrasse 5-13 (Haus D), 81377 München, Germany
[2] Institut für Anorganische und Analytische Chemie, Universität Münster, Corrensstrasse 30, D-48149 Münster, Germany

E-mail: johrendt@lmu.de

Abstract
The structural and magnetic phase transitions of the ternary iron arsenides SrFe$_2$As$_2$ and EuFe$_2$As$_2$ were studied by temperature-dependent x-ray powder diffraction and ^{57}Fe Mössbauer spectroscopy. Both compounds crystallize in the tetragonal ThCr$_2$Si$_2$-type structure at room temperature and exhibit displacive structural transitions at 203 K (SrFe$_2$As$_2$) and 190 K (EuFe$_2$As$_2$), respectively, to orthorhombic lattice symmetry in agreement with the group–subgroup relationship between $I4/mmm$ and $Fmmm$ (β-SrRh$_2$As$_2$-type). ^{57}Fe Mössbauer spectroscopy experiments with SrFe$_2$As$_2$ show full hyperfine field splitting below the phase transition temperature (8.91(1) T at 4.2 K). Order parameters were extracted from detailed measurements of the lattice parameters and fitted to a simple power law. We find a relation between the critical exponents and the transition temperatures for AFe$_2$As$_2$ compounds, which shows that the transition of BaFe$_2$As$_2$ is indeed more continuous than the transition of SrFe$_2$As$_2$, but it remains second order even in the latter case.

(Some figures in this article are in colour only in the electronic version)

1. Introduction

The discovery of the iron arsenide superconductors has provided fresh impetus in the field of high-T_C superconductivity [1, 2]. LaFeAsO with the tetragonal ZrCuSiAs-type structure [3] becomes superconducting by doping the (FeAs)$^{\delta-}$ layers either with electrons or holes [4, 5]. The initially reported transition temperature of 26 K was quickly increased to 55 K by replacing La^{3+} ions by smaller Sm^{3+} ions [6]. The crystal structure of LaFeAsO contains alternating layers of edge-sharing La$_{4/4}$O and FeAs$_{4/4}$ tetrahedra and superconductivity emerges in the FeAs layers by adding or removing about 0.2 electrons per formula unit.

Very recently we reported on the oxygen-free iron arsenide BaFe$_2$As$_2$ with the ThCr$_2$Si$_2$-type structure as another possible parent compound for superconductivity [7]. Soon after that we were able to induce superconductivity by hole doping in the compound (Ba$_{0.6}$K$_{0.4}$)Fe$_2$As$_2$ with T_C = 38 K and we have therefore established a further family of iron arsenide superconductors [8]. Another report on superconductivity at 37 K in isostructural K- and Cs-doped SrFe$_2$As$_2$ followed quickly [9]. The crystal structures of both LaFeAsO and BaFe$_2$As$_2$ are depicted in figure 1. Both compounds are built up by almost identical (FeAs)$^{\delta-}$ layers, but they are separated by lanthanum oxide sheets in LaFeAsO and by barium atoms in BaFe$_2$As$_2$.

The non-superconducting parent compounds LaFeAsO and BaFe$_2$As$_2$ show remarkably similar properties. Both are poor metals and only weakly magnetic. One key finding is the existence of a spin-density-wave (SDW) anomaly,
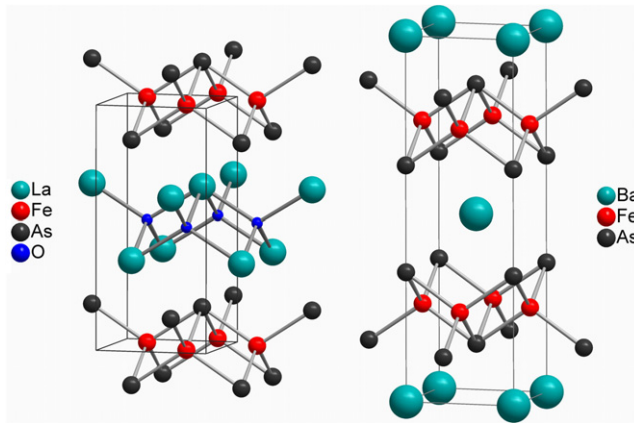
Figure 1. Crystal structures of LaFeAsO and BaFe$_2$As$_2$.

which occurs at T_{tr} = 150 K in LaFeAsO and at T_{tr} = 140 K in BaFe$_2$As$_2$ [10, 7]. This SDW is linked to abrupt changes in the electrical resistivity and magnetic susceptibility and also to structural phase transitions. Antiferromagnetic ordering was found in LaFeAsO 18 K below the structural transition [10], but directly at or at least very close to the lattice distortion temperature in BaFe$_2$As$_2$ according to recent neutron diffraction experiments [11]. It is currently believed that superconductivity in the iron arsenides is intimately connected with the suppression of this SDW anomaly by doping. This suggests that spin-fluctuations may play an important role in the mechanism of superconductivity as was also assumed for the high-T_C cuprates. Thus, the nature of the phase transitions is important for a deeper understanding of superconductivity in the iron arsenides. However, precise structural data close to the phase transition are only available for BaFe$_2$As$_2$ and LaFeAsO [7, 12, 13]. SrFe$_2$As$_2$ has been studied with single crystal data of relatively low resolution [14], which do not allow evaluation of the order parameter close to the transition temperature. Furthermore, the connection between the structural transition in SrFe$_2$As$_2$ and magnetic ordering as well as the structure of EuFe$_2$As$_2$ at low temperatures, have not been investigated yet. We have therefore studied the structural phase transitions of polycrystalline SrFe$_2$As$_2$ and EuFe$_2$As$_2$ in detail by temperature-dependent x-ray powder diffraction. We could also confirm the association of the structural transition in SrFe$_2$As$_2$ with magnetic ordering by ^{57}Fe Mössbauer spectroscopy.

2. Experimental details

SrFe$_2$As$_2$ and EuFe$_2$As$_2$ were synthesized by heating mixtures of distilled Sr(Eu) metal, iron powder and sublimed arsenic at ratios of 1:2:2 in alumina crucibles, which were sealed in silica tubes under an atmosphere of purified argon. The mixtures were heated to 850 K at a rate of 50 K h^{-1}, kept at this temperature for 15 h and cooled down to room temperature. The reaction products were homogenized in an agate mortar, pressed into pellets and annealed at 900 K for 15 h. The obtained black crystalline powders of SrFe$_2$As$_2$ and EuFe$_2$As$_2$ are sensitive to air and moisture.
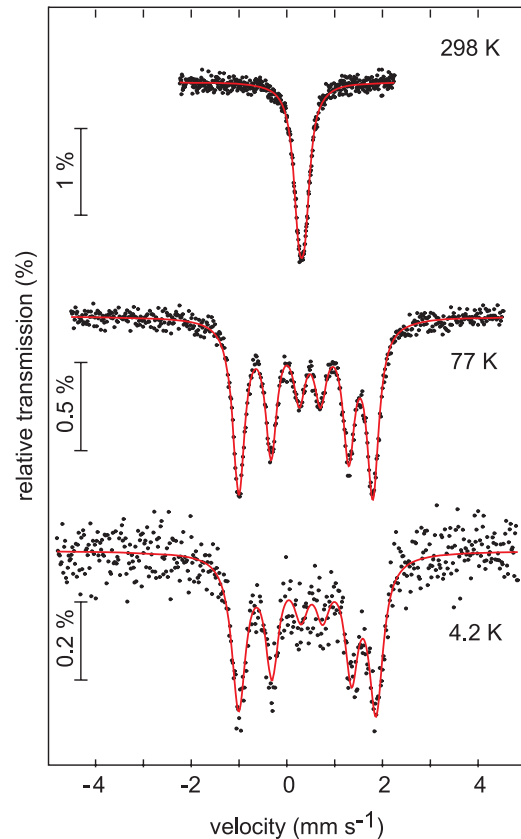

Figure 2. ^{57}Fe Mössbauer spectra of SrFe$_2$As$_2$ with transmission integral fits.

Temperature-dependent x-ray powder diffraction data were collected using a HUBER G670 Guinier imaging plate diffractometer (Cu-Kα_1 radiation, Ge-111 monochromator), equipped with a closed-cycle He-cryostat. Rietveld refinements were performed with the GSAS package [15] using Thompson–Cox–Hastings functions [16] with asymmetry corrections as reflection profiles [17].

A ^{57}Co/Rh source was available for the ^{57}Fe Mössbauer spectroscopic investigations. The velocity was calibrated relative to the signal of α-Fe. A SrFe$_2$As$_2$ sample was placed in a thin-walled PVC container at a thickness of about 4 mg Fe cm^{-2}. The measurements were performed in the usual transmission geometry at 298, 77 and 4.2 K. The source was kept at room temperature.

3. Results and discussion

In order to clarify the connection between the structural phase transition in SrFe$_2$As$_2$ and magnetic ordering, we first present ^{57}Fe Mössbauer spectra of SrFe$_2$As$_2$ measured at 298, 77 and 4.2 K, respectively (figure 2) together with transmission integral fits. In agreement with the ThCr$_2$Si$_2$-type crystal structure we observed a single absorption line for SrFe$_2$As$_2$. At 77 K, which is well below the structural transition temperature, we detected full magnetic hyperfine splitting of the signal. Excellent fits of the data were obtained with the parameters listed in table 1. The isomer shifts are similar to those
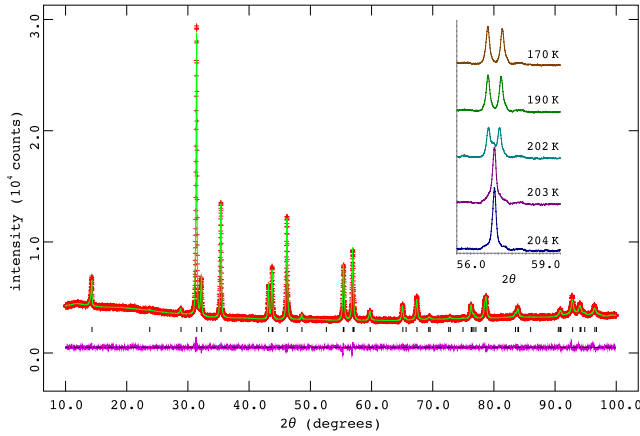
Figure 3. X-ray powder pattern measured at 297 K $(+)$ and Rietveld fit $(-)$ of $SrFe_2As_2$. Inset: splitting of the (2 1 3) reflection.

Table 1. Fitting parameters of ^{57}Fe Mössbauer spectroscopy measurements with $SrFe_2As_2$: δ, isomer shift; ΔE_Q, quadrupole splitting parameter; Γ, experimental line width; B_{hf}, magnetic hyperfine field.

T (K)	δ (mm s^{-1})	Γ (mm s^{-1})	ΔE_Q (mm s^{-1})	B_{hf} (T)
298	0.31(1)	0.28(1)	$-0.13(1)$	—
77	0.44(1)	0.31(1)	$-0.09(1)$	8.70(1)
4.2	0.47(1)	0.37(6)	$-0.09(1)$	8.91(1)

found in $BaFe_2As_2$ ($\delta = 0.31$–0.44 mm s^{-1}) [7]. Due to different ionic radii, we observed a smaller c/a ratio of 3.15 for $SrFe_2As_2$ in comparison to $c/a = 3.29$ for $BaFe_2As_2$ [18]. The stronger compression of the $FeAs_{4/4}$ tetrahedra in the strontium compound is also reflected by the larger quadrupole splitting parameter. This is in good agreement with the recently published ^{57}Fe data for LaFePO [19] and LaFeAsO [20, 21], which contain electronically very similar tetrahedral $FeP_{4/4}$ and $FeAs_{4/4}$ layers. The hyperfine field detected at the iron nuclei in $SrFe_2As_2$ ($B_{hf} = 8.91(1)$ T) at 4.2 K is considerably higher than in $BaFe_2As_2$ (5.47 T) [7]. The magnetic behavior of the iron arsenide layers strongly depends on the occupation of the Fe $3d_{x^2-y^2}$ orbitals, and the latter depends on the position of the arsenic atoms [22]. Thus, with smaller strontium and europium atoms, a stronger magnetism of the iron arsenide layers and consequently a higher ordering temperature can be observed, i.e. 140 K in $BaFe_2As_2$, 205 K in $SrFe_2As_2$ [22] and 200 K in $EuFe_2As_2$ [23]. The hyperfine fields show the same trend: 5.47 T in $BaFe_2As_2$ [7], 8.91 T K in $SrFe_2As_2$ and 8.5 T in $EuFe_2As_2$ [23].

According to recently published single crystal data [14], $SrFe_2As_2$ exhibits a structural transition from the tetragonal space group $I4/mmm$ to the orthorhombic subgroup $Fmmm$ according to the β-$SrRh_2As_2$-type structure [24] as described for $BaFe_2As_2$ [7]. Anomalies of the physical properties have been reported for polycrystalline $SrFe_2As_2$ at 205 K [22] and at 198 K for single crystals [14]. We can confirm a structural transition at 203 K by x-ray powder patterns at low temperatures. Figure 3 shows the experimental and fitted powder pattern of $SrFe_2As_2$ at room temperature. The inset

Table 2. Crystallographic data for low-temperature $SrFe_2As_2$ and $EuFe_2As_2$.

	$SrFe_2As_2$	$EuFe_2As_2$
Temperature (K)	90	10
Space group	$Fmmm$	$Fmmm$
a (pm)	557.83(3)	555.46(2)
b (pm)	551.75(3)	549.83(2)
c (pm)	1229.65(6)	1205.90(4)
V (nm^3)	0.37846(1)	0.36830(4)
Z	4	4
ρ_{calc} (g cm^{-3})	6.11	7.46
Data points	5823	7650
Reflections (all phases)	145	306
Atomic parameters	5	5
Profile parameters	4	10
Background parameters	36	36
Other parameters	12	24
d range	0.963–6.148	0.945–7.681
R_P, wR_P	0.0361, 0.0487	0.0131, 0.0237
$R(F^2)$, $\chi 2$	0.104, 4.444	0.064, 2.371
GooF	2.11	1.54
Atomic parameters:		
Sr, Eu	$4a$ (0, 0, 0)	$4a$ (0, 0, 0)
	$U_{iso} = 180(40)$	$U_{iso} = 73(6)$
Fe	$8f$ ($\frac{1}{4}$, $\frac{1}{4}$, $\frac{1}{4}$)	$8f$ ($\frac{1}{4}$, $\frac{1}{4}$, $\frac{1}{4}$)
	$U_{iso} = 60(20)$	$U_{iso} = 47(6)$
As	$8i$ (0, 0, z)	$8i$ (0, 0, z)
	$z = 0.3612(3)$	$z = 0.3632(1)$
	$U_{iso} = 60(20)$	$U_{iso} = 87(6)$
Bond lengths (pm):		
(Sr, Eu)–As	$324.4(3) \times 4$	$320.6(1) \times 4$
	$327.0(3) \times 4$	$323.0(1) \times 4$
Fe–As	$239.1(3) \times 4$	$238.3(1) \times 4$
Fe–Fe	$278.9(1) \times 2$	$277.7(1) \times 2$
	$275.9(1) \times 2$	$274.9(1) \times 2$
Bond angles (deg):		
As–Fe–As	$110.2(2) \times 2$	$110.1(1) \times 2$
	$109.5(1) \times 2$	$109.6(1) \times 2$
	$108.6(1) \times 2$	$108.7(1) \times 2$

shows a clearly discernable splitting of the (2 1 3)-reflection which was observed below 203 K. We refined the structures at room temperature and well below the transition temperature, the obtained crystallographic data are summarized in tables 2 and 3.

An intensively discussed question is whether the transition is of first or second order. For second order transitions, the space groups of the distorted and undistorted structures have to comply with a group–subgroup relationship according to Hermann's theorem [25, 26]. The space group $Fmmm$ is a *translationengleiche* subgroup of $I4/mmm$ of index 2. Thus, from a group theoretical standpoint one could expect a second order transition with continuous variation of the order parameter.

Figure 4 shows the unit cell parameters of $SrFe_2As_2$ determined by Rietveld refinements. The a lattice parameter in the tetragonal structure has been multiplied by $\sqrt{2}$ for better comparison. We found a rather abrupt splitting of the lattice parameters on cooling below 203 K. The tetragonal axis $a_t = 555.11$ pm splits by $+2.0$ pm ($+0.365\%$) and -1.9 pm (-0.343%) within 1 K, leading to $a_o = 557.13(3)$ pm and $b_o = 553.20(3)$ pm at 202 K. Below this temperature, we
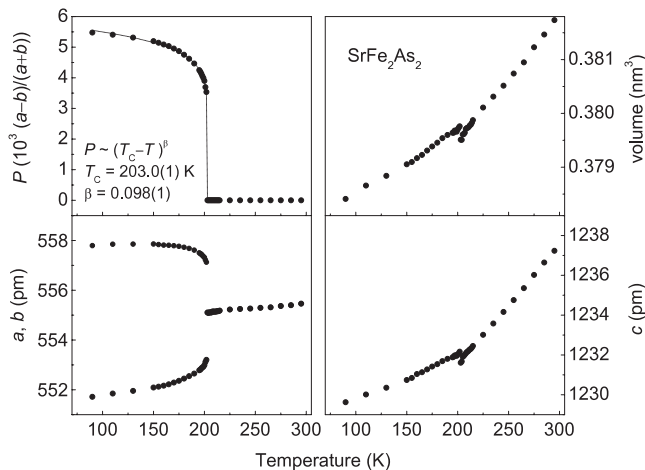
3

Figure 4. Lattice parameters, cell volume and order parameter of $SrFe_2As_2$. The line describes the power-law fit. Error bars are within data points.

Figure 5. X-ray powder pattern measured at 297 K (+) and Rietveld fit (−) of $EuFe_2As_2$. FeAs (<20%) and Eu_2O_3 (<1%) were included as minor impurity phases. Inset: splitting of the (2 1 3) reflection.

Table 3. Crystallographic data for $SrFe_2As_2$ and $EuFe_2As_2$ at 297 K.

	$SrFe_2As_2$	$EuFe_2As_2$
Space group	$I4/mmm$	$I4/mmm$
a (pm)	392.43(1)	390.62(1)
b (pm)	$=a$	$=a$
c (pm)	1236.44(1)	1212.47(2)
V (nm^3)	0.19041(1)	0.18501(1)
Z	2	2
ρ_{calc} (g cm^{-3})	6.09	7.42
Data points	9000	7800
Reflections (all phases)	46	281
Atomic parameters	4	4
Profile parameters	8	8
Background parameters	36	36
Other parameters	5	20
d range	0.981–6.182	0.960–7.678
R_P, wR_P	0.0232, 0.0306	0.0147, 0.0209
$R(F^2)$, $\chi 2$	0.029, 1.601	0.047, 2.580
GooF	1.27	1.61
Atomic parameters:		
Sr, Eu	$2a$ (0, 0, 0)	$2a$ (0, 0, 0)
	$U_{iso} = 129(5)$	$U_{iso} = 123(5)$
Fe	$4d$ ($\frac{1}{2}$, 0, $\frac{1}{4}$)	$4d$ ($\frac{1}{2}$, 0, $\frac{1}{4}$)
	$U_{iso} = 72(4)$	$U_{iso} = 91(6)$
As	$4e$ (0, 0, z)	$4e$ (0, 0, z)
	$z = 0.3600(1)$	$z = 0.3625(1)$
	$U_{iso} = 86(4)$	$U_{iso} = 96(5)$
Bond lengths (pm):		
(Sr, Eu)–As	$327.0(1) \times 8$	$322.6(1) \times 8$
Fe–As	$238.8(1) \times 4$	$238.2(1) \times 4$
Fe–Fe	$277.5(1) \times 4$	$276.2(1) \times 2$
Bond angles (deg):		
As–Fe–As	$110.5(1) \times 2$	$110.1(1) \times 2$
	$108.9(1) \times 4$	$109.1(1) \times 2$

observed a continuous increase of a_o and a decrease of b_o. (a_o) saturates at 165 K towards a total change of +0.67%, whereas (b_o) decreases further to a total change of −0.94% at 90 K. The different behavior of the orthorhombic axis is most likely a consequence of the magnetic ordering involved in the structural transition. We can understand this anisotropy if we
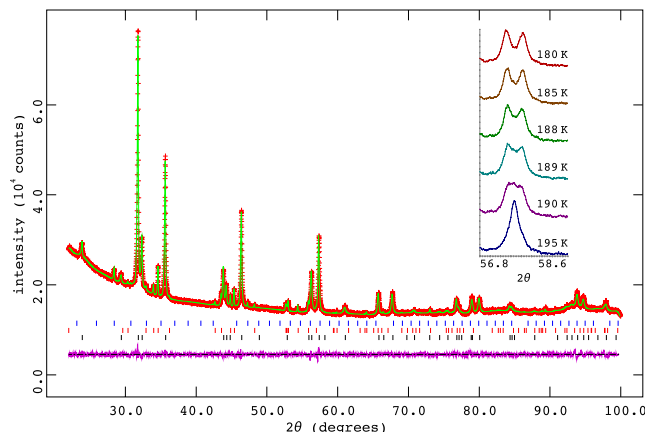
assume that the spin moments at the iron atoms in $SrFe_2As_2$ are aligned parallel to *one* orthorhombic axis and perpendicular to the other one, as known for LaFeAsO [10] and recently reported for $BaFe_2As_2$ [11].

The temperature dependence of the order parameter $P = \frac{a-b}{a+b}$ is presented in figure 4. We can fit the data to a power law $P = q(\frac{T_{tr}-T}{T})^\beta$ to obtain the critical exponent $\beta = 0.098(1)$ and the critical temperature $T_{tr} = 203.0(1)$ K. Simple power-law dependencies defining critical exponents are generally valid close to the critical point, but the values of the critical exponents are often very different from the Landau prediction ($\beta = \frac{1}{2}$). However, it is well known that the Landau theory fails to provide a general description of critical phenomena. In the present case, the two-dimensional character of the structure has to be taken into account and the exponent $\beta \approx 0.1$ is not too far from $\frac{1}{8}$, which is the prediction of the two-dimensional Ising model [27, 28].

So far, the structural transition of $SrFe_2As_2$ has a clear signature of second order, but on the other hand some results point to a first order mechanism. Typical signs for first order transitions are the occurrence of hysteresis and a volume jump at T_{tr}. Indeed, specific heat measurements [22] show a hysteresis of ≈0.2 K. This value is unexpectedly small, but quite consistent with our results regarding the cell volume. We find a jump at T_{tr} as discernible from the volume plot in figure 4, but the value $\frac{\Delta V}{V}$ is only 0.07%. This is extremely small, especially if we keep in mind that the changes in the a and b lattice parameters are around 1%. We do not believe that this very small hysteresis and volume jump clearly prove a first order transition mechanism.

This point of view is supported by a comparison between the structural data for $SrFe_2As_2$ and those of other AFe_2As_2 compounds. Figure 5 shows the Rietveld fit of the $EuFe_2As_2$ sample. Crystallographic data for the ambient and low-temperature structures are compiled in tables 2 and 3. In figure 6 we present the lattice and order parameters of $EuFe_2As_2$. We were not able to determine the exact progression of the c axis and thus the volume in the proximity of T_{tr}. A behavior very similar to $SrFe_2As_2$ is observed, but T_{tr}
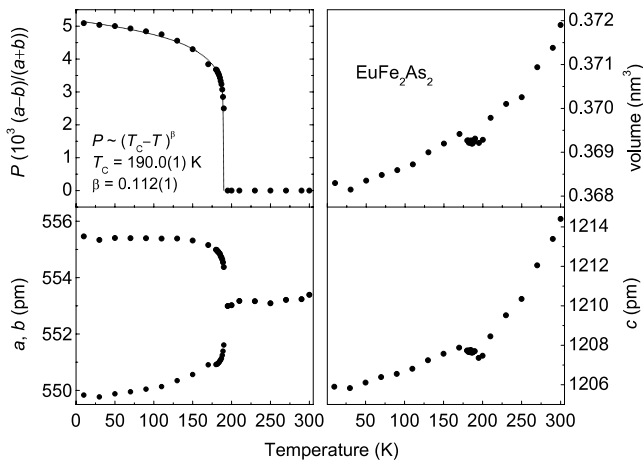
Figure 6. Lattice parameters, cell volume and order parameter of EuFe$_2$As$_2$. The line describes the power-law fit. Error bars are within data points.

decreases to 190.0(1) K and the critical exponent increases to $\beta = 0.112(1)$. This trend continues in the case of BaFe$_2$As$_2$ with $T_{tr} = 139$ K and $\beta = 0.142$ [7]. Obviously, the critical exponent β scales with T_{tr} and the transition indeed converges towards first order (where β vanishes), but remains second order even in SrFe$_2$As$_2$. This is also what to expect from group theory. It is worth mentioning that the abruptness of a phase transition is by no means a cast-iron argument for a first order mechanism. This is, however, a question of data accuracy close to the critical point.

4. Conclusion

In summary, our results suggest a complex nature of the phase transitions in AFe$_2$As$_2$ compounds due to several competing order parameters with respect to their structural and magnetic components. We have shown by Mössbauer spectroscopy that the transition of SrFe$_2$As$_2$ is accompanied by magnetic ordering as is the case for the Ba and Eu compounds. We are aware that the magnetic ordering is coupled to the lattice and that both contributions are hard to distinguish due to their proximity. However, the focus in the current work has been on the structural part. Our precise determination of the lattice parameters close to T_{tr} are indicative of a second order transition with continuous varying order parameters and simple power-law dependencies for both SrFe$_2$As$_2$ and EuFe$_2$As$_2$. This is typical for displacive structural transitions and consistent with the group–subgroup relationship between the $I4/mmm$ and $Fmmm$ space groups. The comparison between the data for SrFe$_2$As$_2$, EuFe$_2$As$_2$ and BaFe$_2$As$_2$ clearly reveals a relation between the transition temperatures and the critical exponents. Obviously, the transition becomes

more and more continuous as T_{tr} decreases from SrFe$_2$As$_2$ towards BaFe$_2$As$_2$. But of course, the mechanism is the same in all three cases. From this we conclude that all AFe$_2$As$_2$ compounds with A = Ba, Sr and Eu undergo second order displacive structural transitions.

References

[1] Kamihara Y, Watanabe T, Hirano M and Hosono H 2008 *J. Am. Chem. Soc.* **130** 3296–7
[2] Johrendt D and Pöttgen R 2008 *Angew. Chem. Int. Edn* **47** 4782–4
[3] Johnson V and Jeitschko W 1974 *J. Solid State Chem.* **11** 161–6
[4] Lu W 2008 *Solid State Commun.* **148** 168
[5] Wen H-H, Mu G, Fang L, Yang H and Zhu X 2008 *Europhys. Lett.* **82** 17009
[6] Ren Z *et al* 2008 *Chin. Phys. Lett.* **25** 2215
[7] Rotter M, Tegel M, Johrendt D, Schellenberg I, Hermes W and Pöttgen R 2008 *Phys. Rev.* B **78** 020503(R)
[8] Rotter M, Tegel M and Johrendt D 2008 *Phys. Rev. Lett.* **101** 107006
[9] Sasmal K, Lv B, Lorenz B, Guloy A M, Chen F, Xue Y and Chu C 2008 *Phys. Rev. Lett.* **101** 107007
[10] de la Cruz C *et al* 2008 *Nature* **453** 899
[11] Huang Q, Qiu Y, Bao W, Lynn J W, Green M A, Chen Y, Wu T, Wu G and Chen X H 2008 arXiv:0806.2776
[12] Nomura T, Kim S W, Kamihara Y, Hirano M, Sushko P V, Kato K, Takata M, Shluger A L and Hosono H 2008 arXiv:0804.3569
[13] McGuire M A *et al* 2008 arXiv:0806.3878
[14] Yan J-Q *et al* 2008 *Phys. Rev.* B **78** 024516
[15] Larson A C and Von Dreele R B 2004 General Structure Analysis System *Los Alamos Laboratory Report LAUR 86*
[16] Thompson P, Cox D E and Hastings J B 1987 *J. Appl. Crystallogr.* **20** 79–83
[17] Finger L W, Cox D E and Jephcoat A P 1994 A correction for powder diffraction peak asymmetry due to axial divergence *J. Appl. Crystallogr.* **27** 892–900
[18] Pfisterer M and Nagorsen G 1980 *Z. Naturforsch.* B **35** 703–4
[19] Tegel M, Schellenberg I, Pöttgen R and Johrendt D 2008 *Z. Naturforsch.* B **63** 1057–61
[20] Kitao S, Kobayashi Y, Higashitanguchi S, Saito M, Kamihara Y, Hirano M, Mitsiu T, Hosono H and Seto M 2008
[21] Klauss H-H *et al* 2008 *Phys. Rev. Lett.* **101** 077005
[22] Krellner C, Caroca-Canales N, Jesche A, Rosner H, Ormeci A and Geibel C 2008 *Phys. Rev.* B **78** 100504
[23] Raffius H, Mörsen E, Mosel B D, Müller-Warmuth W, Jeitschko W, Terbüchte L and Vomhof T 1993 *J. Phys. Chem. Solids* **54** 135
[24] Hellmann A, Löhken A, Wurth A and Mewis A 2007 *Z. Naturforsch.* B **62** 155
[25] Hermann C 1929 *Z. Kristallogr.* **69** 533
[26] Deonarine S and Birman J L 1983 *Phys. Rev.* B **27** 4263–73
[27] Lines M E and Glass A M 1977 *Principles and Applications of Ferroelectrics and Related Materials* (Oxford: Clarendon)
[28] Stanley H E 1971 *Introduction to Phase Transitions and Critical Phenomena* (Oxford: Clarendon)